Progress In Electromagnetics Research Letters, Vol. 111, 111–120, 2023

Wideband Circular Polarized Fractal Antenna for RFID/WiMAX/WLAN Applications

En Cheng Wang[1], Xiu Feng Liu[1, *], and Hu Chang[2]

Abstract—A novel wideband circularly polarized (CP) dipole antenna for RFID/WiMAX/WLAN applications is presented. A pair of crossed fan-shaped dipoles printed on both sides of the substrate are used as the primary radiating elements. The antenna achieves circular polarization by using a 90° phase shifted microstrip line between the dipoles. By changing the edge of fan dipoles into Minkowski fractal curve, miniaturization and wide bandwidth of the antenna can be realized. Besides, incorporating the U-slot into the fractal crossed dipoles can obtain a wider bandwidth. The test results show that the proposed antenna achieves a wide impedance bandwidth of 63.2% (1.9–3.7 GHz) for VSWR < 2 and a 3-dB axial ratio (AR) bandwidth of 42.9% (2.2–3.4 GHz). The maximum gain in the operating frequency band can reach 7 dBi. The proposed antenna has good radiation characteristics in both low and high frequencies, which makes it a candidate for applications of RFID, WLAN, WiMAX, and other communication systems.

1. INTRODUCTION

Circularly polarized (CP) antennas are widely employed in navigation, radio frequency identification (RFID), wireless local network (WLAN), Worldwide Interoperability for Microwave Access (WiMAX), and other communication systems due to their inherent advantage of insensitivity to depolarization [1, 2]. When electronic devices meeting different needs are concentrated on the same carrier, a complex electromagnetic environment will be formed, and the performance indexes of different antennas will be reduced due to strong near-field coupling. Using broadband antennas can reduce the interference between antennas. However, CP antennas usually suffer limitations including the achievable impedance and axial-ratio (AR) bandwidths. Up to now, many methods have been proposed to broaden the impedance and AR bandwidths. A CP antenna is presented in [3], which uses a coplanar waveguide-feed to obtain broadband, but its bidirectional radiation property leads to low gain. The external polarizers such as Wilkinson power divider or hybrid coupler can also expand the antenna bandwidth [4, 5]. However, such ways will not only complicate the manufacture of the antenna but also increase the antenna size. A broadband cross-dipole antenna with a sequentially rotated configuration has been proposed in [6], using a pair of vacant-quarter rings to connect the dipoles as a feeding structure to achieve wideband CP. In recent years, some research on metasurface is also enlightening [7, 8].

Many studies have shown that fractal geometry concept can be applied to the design of antennas to achieve small size, wide bandwidth, and higher gain [9–11]. In addition, etching a U-slot has been demonstrated as an effective way to broaden bandwidth and reduce size in some reports [12–14].

In this paper, a wideband CP cross-dipole antenna is presented. A sequential rotating structure is used to generate CP. By changing the boundary of the cross-dipole into a fractal structure and incorporating U-slot on it, the antenna size is effectively reduced while the bandwidth is broadened. The

Received 26 March 2023, Accepted 8 July 2023, Scheduled 28 July 2023

* Corresponding author: Xiufeng Liu (2225678039@qq.com).

[1] School of Information Engineering, North China University of Technology, Beijing 100144, China. [2] State Grid Huainan Power Supply Company of Anhui Province, Huainan 232000, China.

antenna is simulated by the ANSYS High-Frequency Structure Simulator (HFSS), and its performance is verified by measurements. Experiment results reveal that the proposed design achieves a wide impedance bandwidth of 63.2% (1.9–3.7 GHz) for voltage standing wave ratio (VSWR) < 2 and a 3-dB AR bandwidth of 42.9% (2.2–3.4 GHz). The gain in impedance bandwidth is higher than 5 dBi.

2. ANTENNA DESIGN

Figure 1 shows the geometry of the proposed antenna. The antenna is composed of two printed dipoles with fractal boundaries, a reflecting plate, a curved-delay line, and a semi-rigid coaxial line. The printed crossed dipole is suspended at a height H from the reflecting plate, which is fabricated on both sides of an FR4 substrate with a thickness HS of 1.6 mm, a relative permittivity of 4.4, and a loss tangent of 0.02. One-half of the dipole is printed on top of the substrate, while the other half is on the bottom. The upper dipole and bottom dipole rotate 180° around the center of the substrate. The edge of dipole is modified to a fractal structure based on Minkowski fractal curve. Minkowski curve is a notable fractal geometry, which has been used widely in telecommunication systems antennas. By adjusting the shape and order of the Minkowski curve, the bandwidth, gain, and circular polarization of the antenna can be changed to meet the design requirements. The geometric construction of the proposed fractal shape is shown in Fig. 2. The fractal structure is stepped, and the same stepped curve is continuously constructed on each side. A third-order fractal structure is constructed, which is used on the boundaries of the proposed antenna to provide good performance in bandwidth.

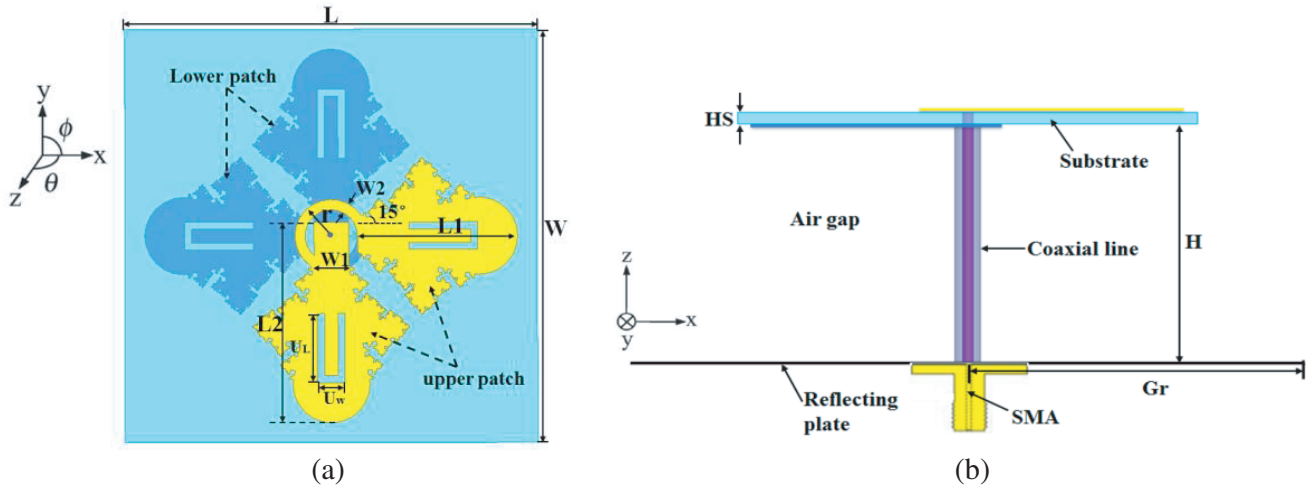

Figure 1. Geometry of this antenna. (a) Top view. (b) Side view.

The antenna is center-fed by a 50 Ω semi-rigid coaxial line to achieve symmetric CP radiation patterns across the entire operating bandwidth. The outer conductor of the semi-rigid coaxial line is connected with the lower dipole patch, and the inner core is connected with the upper dipole patch through a drilled hole in the substrate. The length of the semi-rigid coaxial line is approximately $\lambda 0/4$ ($\lambda 0$ refers to the center frequency of operation). As the length $\lambda 0/4$ of the coaxial line would cancel an induced current of the outer sides of the coaxial line, the proposed dipole can excite the balanced mode without a balun element. In principle, an open circuit is produced at the point connection between the dipole and the coaxial line, which is produced by the distance from the short circuit connected between the reflecting plate and the shield conductor of a coaxial line. This open circuit can avoid generating induced current outside the coaxial line and give and gives balanced operation to an inherently unbalanced transmission line. To excite a right-hand CP radiation, two orthogonal linear polarizations are required. The two orthogonal modes are excited by introducing a 90° phase delay line that comprises a vacant quarter-printed ring, which has a radius of r and a width of $W2$. Due to the sequential phase of dipoles, the proposed antenna can achieve a good CP radiation effect without an

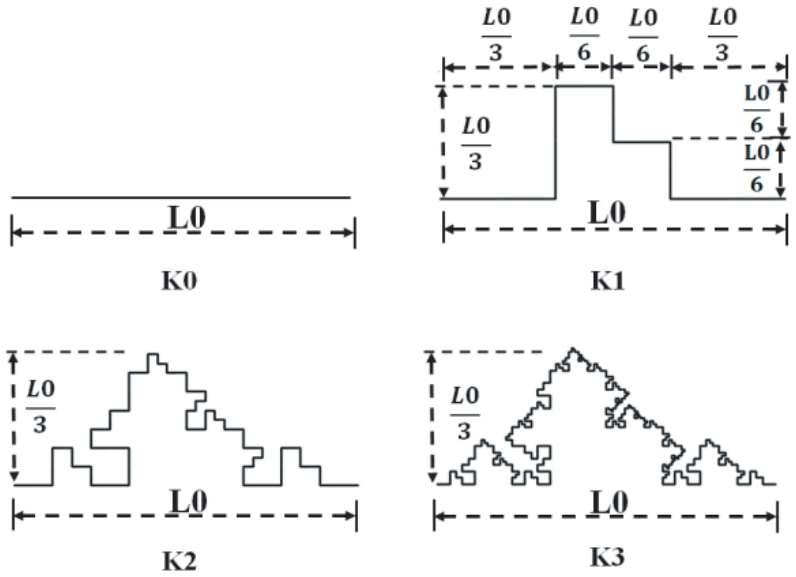

Figure 2. Iterations of the proposed fractal geometry.

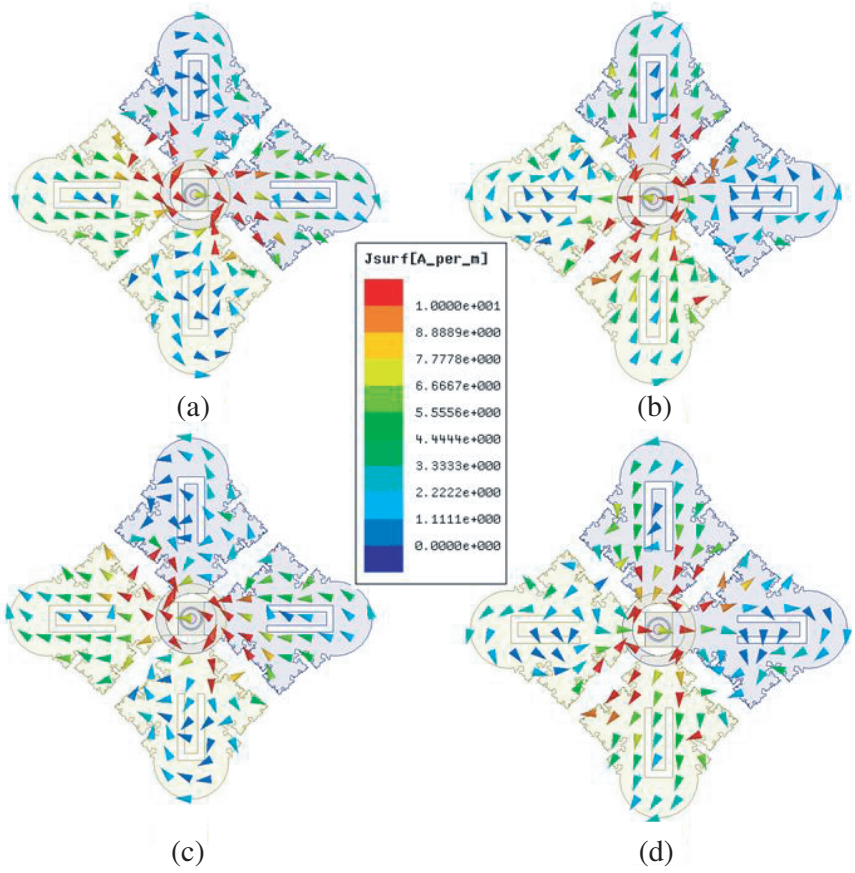

Figure 3. Surface current distribution of antenna at 2.4 GHz. (a) 0°. (b) 90°. (c) 180°. (d) 270°.

external polarizer. To obtain a wider bandwidth, four U-shaped slots are etched on the crossed dipole. A circular reflector with a radius of Gr is selected to obtain good radiation performance.

The current distributions of the proposed antenna at 2.4 GHz are shown in Fig. 3. It is observed

that the currents rotate anticlockwise to yield RHCP (right-hand circular polarization) waves in the bore-sight direction.

3. PARAMETRIC STUDIES

By observing the influence of antenna parameters on antenna performance, the antenna is optimized, and the best antenna parameters are determined. With other conditions being the same, only one parameter is changed at a time.

3.1. Height of the Antenna, H

Figure 4(a) is a comparison of VSWR results with the change of H. It can be seen that the change of H has little effect on VSWR. Fig. 4(b) demonstrates that the antenna height can control the AR at a lower resonant frequency. The AR of the antenna gradually decreases with the increase of H, but at the same time, a certain degree of frequency offset also appears. Therefore, H is determined to be 35 mm.

3.2. Length of the Dipole Arm, L1

Figure 4(c) shows the influence of changing $L1$ on antenna VSWR. With the increase of $L1$, the working bandwidth of the antenna gradually moves to a lower frequency band. Besides, the impedance matching

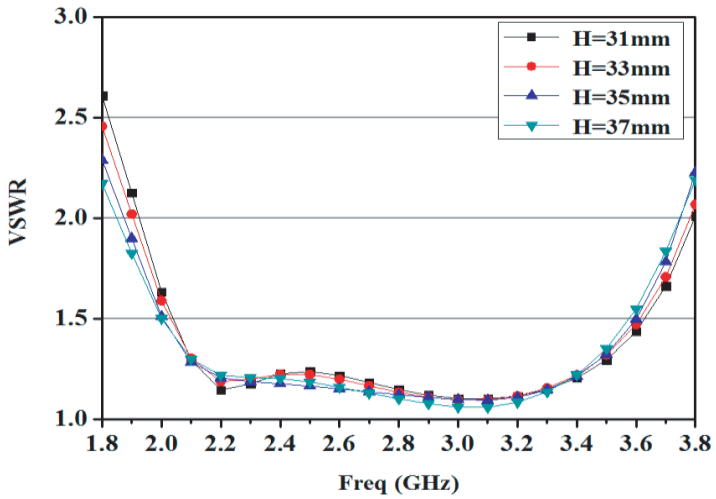

(a)

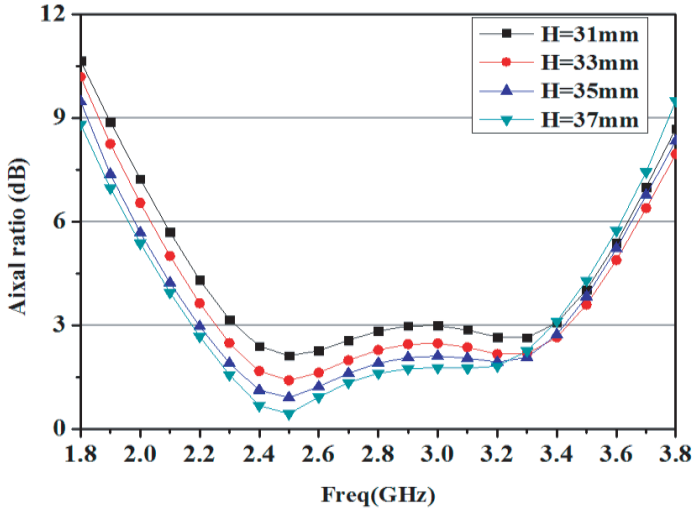

(b)

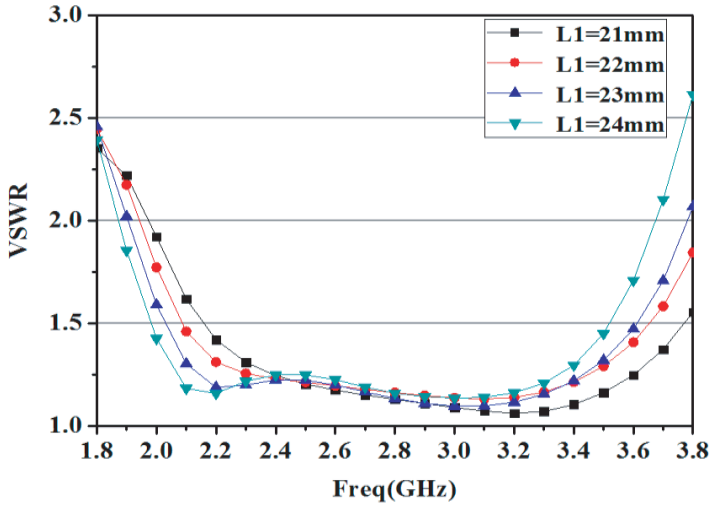
L1=21mm
L1=22mm
L1=23mm
L1=24mm
VSWR
Freq(GHz)
3.0
2.5
2.0
1.5
1.0
1.8
2.0
2.2
2.4
2.6
2.8
3.0
3.2
3.4
3.6
3.8

(c)

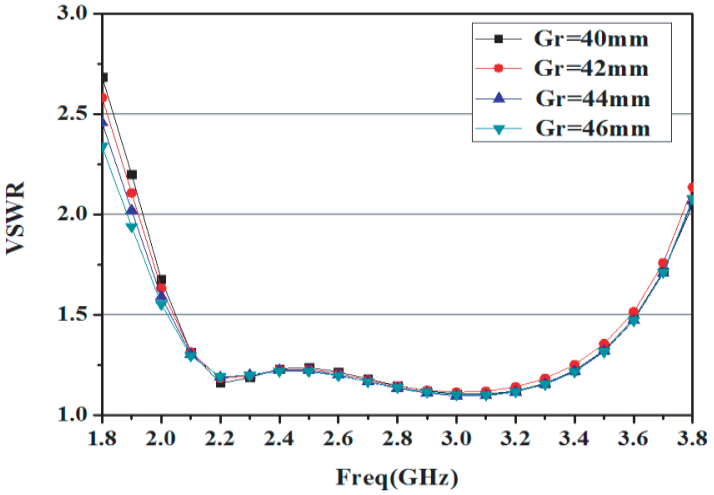
Gr=40mm
Gr=42mm
Gr=44mm
Gr=46mm
VSWR
Freq(GHz)
3.0
2.5
2.0
1.5
1.0
1.8
2.0
2.2
2.4
2.6
2.8
3.0
3.2
3.4
3.6
3.8

(d)

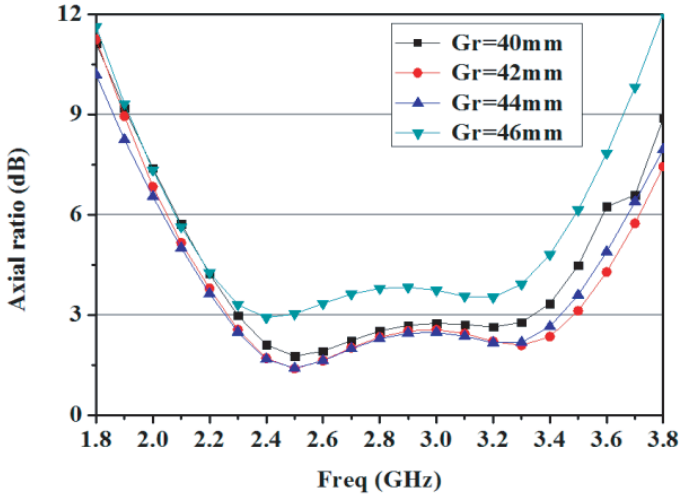
Gr=40mm
Gr=42mm
Gr=44mm
Gr=46mm
Axial ratio (dB)
Freq (GHz)
12
9
6
3
0
1.8
2.0
2.2
2.4
2.6
2.8
3.0
3.2
3.4
3.6
3.8

(e)

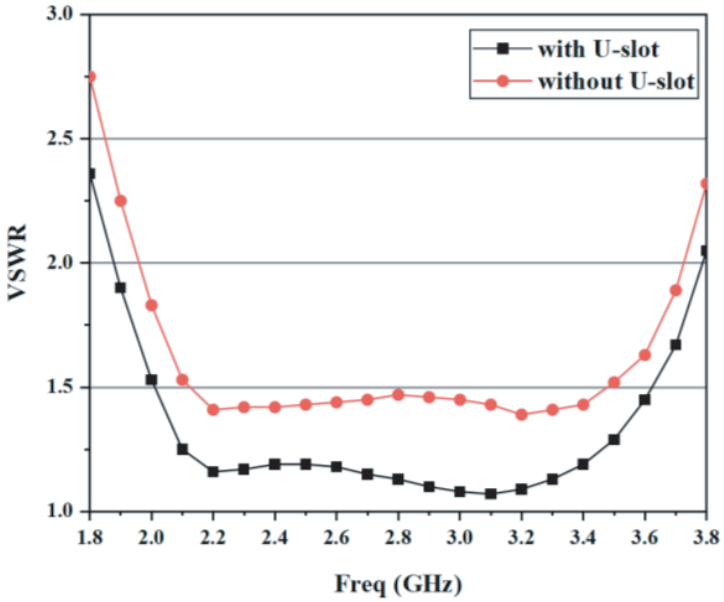

(f)

Figure 4. (a) VSWR variation with different H. (b) AR variation with different H. (c) VSWR variation with different $L1$. (d) VSWR variation with different Gr. (e) AR variation with different Gr. (f) Antenna bandwidth, with or without U-slots.

effect is better when $L1 = 23$ mm, and it meets the requirements of the working frequency band, so the value of $L1$ is determined to be 23 mm.

3.3. Radius of Circular Reflecting Surface, Gr

Figure 4(d) and Fig. 4(e) show the simulated results of VSWR and AR of the antenna when Gr changes from 40 mm to 46 mm. The results display that the variation of Gr has almost no effect on the VSWR of the antenna, but has a significant effect on the AR. When Gr increases from 40 mm to 44 mm, the AR of the antenna decreases, and the CP effect becomes better, but when Gr continues to increase to 46 mm, the AR increases to more than 3 dB, so $Gr = 44$ mm is determined.

3.4. Antenna Bandwidth, with or without U-slots

Figure 4(f) shows the simulated results of antenna bandwidth with or without U-slots. From the results, it can be seen that the impedance bandwidth of the antenna has significantly increased after the use of U-shaped slots. After using a U-shaped slot in the antenna, it can increase the bandwidth by approximately 400 MHz.

4. EXPERIMENTAL VERIFICATION

To validate the simulated results, a prototype of the proposed antenna was fabricated and tested. A photograph of the fabricated antenna is shown in Fig. 5. The VSWR was measured using an Agilent N5230A vector network analyzer. The AR, gain, and radiation pattern of the prototype were measured by a Satimo StarLab system.

Figure 6 shows the simulated and measured results of radiation patterns at 2.45 and 3.2 GHz. The main radiation polarization mode of the antenna is right-handed circular polarization (RHCP), and the radiation patterns are generally symmetrical and exhibit good unidirectional characteristics. The LHCP (left-hand circular polarization) radiation patterns are also listed in the figure for comparison. Fig. 7 shows simulated and measured VSWRs and gains. The measured VSWR is less than 2 over

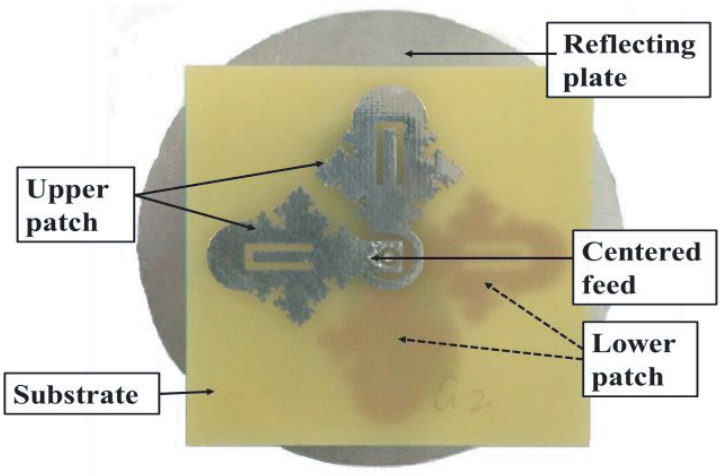

Figure 5. Photographs of the fabricated antenna.

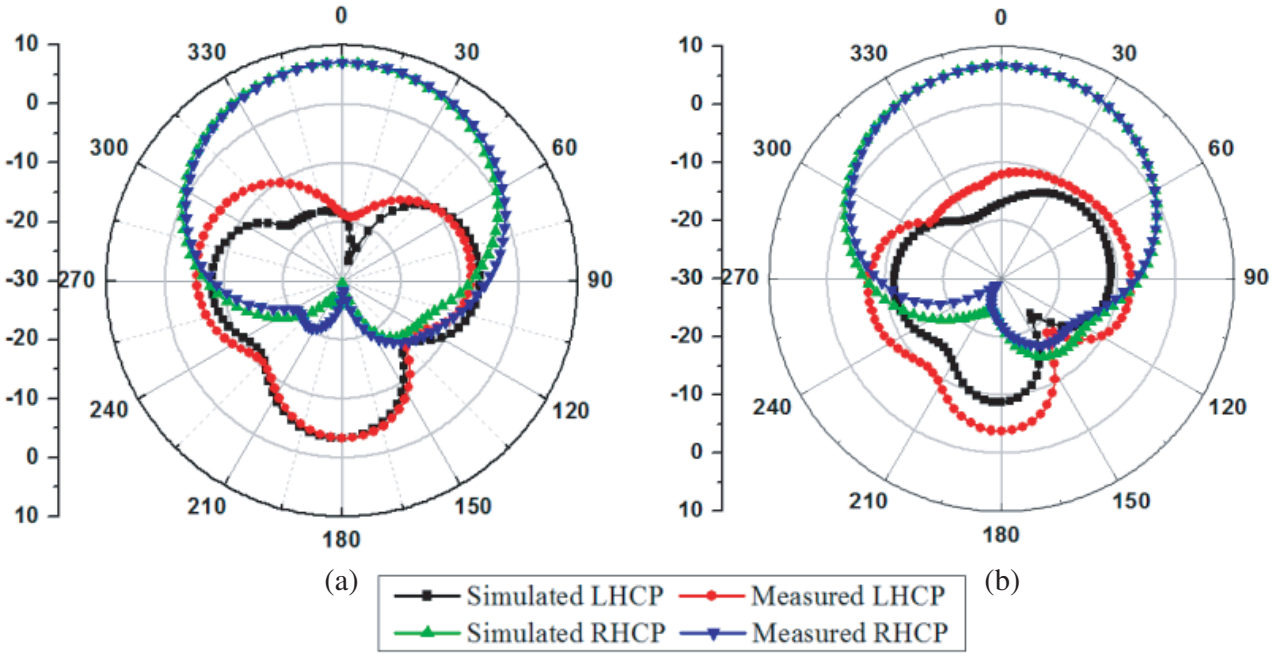

Figure 6. Simulated and measured radiation patterns of the antenna at (a) 2.45 GHz, (b) 3.2 GHz.

Table 1. The 3 dB beamwidth of the antenna at different frequencies.

Frequency (GHz)	HFSS Simulation		Measurement	
	Half power beam width		Half power beam width	
	xz-plane	yz-plane	xz-plane	yz-plane
2.3	80°	80°	81°	81.5°
2.45	80°	80°	80°	80.5°
3.2	86°	85°	86.5°	86°

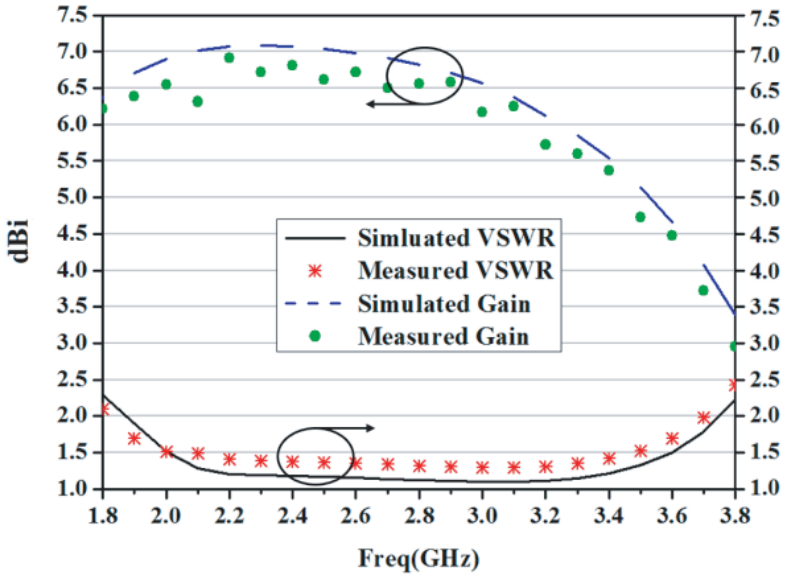

Figure 7. Simulated and Measured VSWR and gain.

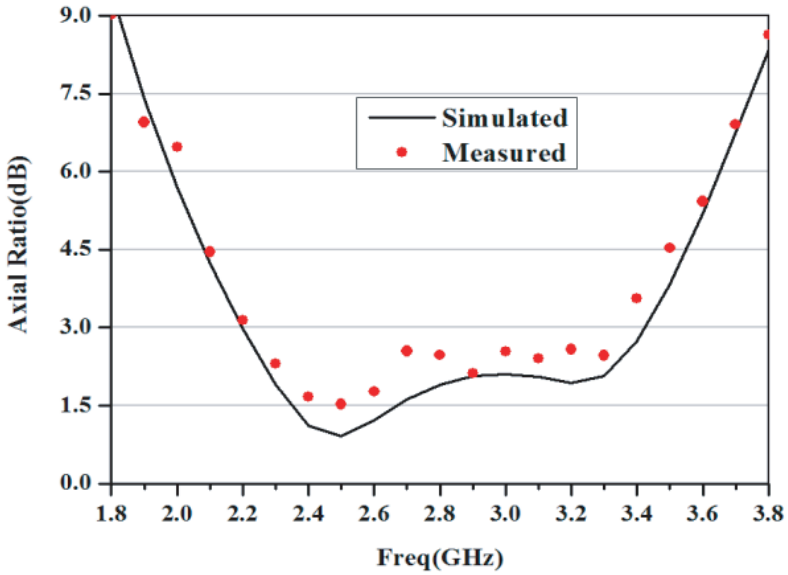

Figure 8. Simulated and Measured axial ratios.

the frequency range of 1.9 to 3.7 GHz, which indicates that the antenna achieves a wide impedance bandwidth. The measured gain is more than 3.5 dBi within the 2 dB VSWR bandwidth and can reach 7 dBi in the working frequency band. Fig. 8 plots the simulated and measured results of the antenna AR. The 3-dB AR bandwidth of the antenna is 42.9% from 2.2 to 3.4 GHz, which is generally covered by the VSWR < 2 operation band. The measured results show good agreement with the simulation. However, due to the roughness of the manufacturing process and the actual loss of materials, some subtle differences may be caused. Better processing techniques may reduce this difference. Table 1 gives a 3 dB beamwidth in the xz- and yz-planes at different frequencies. The initial and optimized parameters of the proposed antenna are listed in Table 2. Table 3 shows the comparison between the proposed antenna and similar antennas. By comparison, the proposed antenna has wider bandwidth, higher gain, and smaller size. The impedance bandwidth of the antenna is 1.9 to 3.7 GHz, as the paper

Table 2. Detailed antenna dimensions.

Parameter	L	W	$L1$	$L2$	r	$W2$	Gr
Value (mm):	52;	52;	21;	23;	4.1;	0.8;	40;
(initial value and the optimized value)	60	60	23	27	5.3	1.5	44
Parameter	$L0$	UL	UW	H	t	HS	
Value (mm):	10;	5;	1;	31;	0.2;	1.0;	
(initial value and the optimized value)	18	10	4	35	1	1.6	

Table 3. Comparison with other antenna.

Ref.	Size (mm)	IMBW (GHz)	ARBW (GHz)	Gain (dBi)
1	$210 \times 210 \times 29$	0.9–0.925/2.43–2.47	0.91–0.95/2.425–2.47	3.1/6.2
3	$206 \times 206 \times 10$	2.35–2.91	2.25–3.25	7.26
5	$150 \times 150 \times 1$	0.78–1	0.86–0.96	2.9
Prop.	$88 \times 88 \times 35$	1.9–3.7	2.2–3.4	7

suggests that the center point of the antenna is at 2.8 GHz. In daily life, most of the carrier frequencies of the communication systems that are often used by people are below 2.8 GHz, so the paper focuses on selecting other commonly used frequency points for testing.

5. CONCLUSIONS

A wideband CP antenna incorporating U-slots into a fractal boundary crossed dipole has been simulated, fabricated, and tested, exhibiting wide 10-dB impedance bandwidth and 3-dB axial-ratio bandwidth. Besides, the antenna has stable and symmetrical radiation patterns and satisfying gain. The proposed antenna has many applications and advantages, promising for RFID, WLAN, WiMAX, and other communication systems.

REFERENCES

1. Sarkar, S. and B. Gupta, "A dual-band circularly polarized antenna with a dual-band AMC reflector for RFID readers," *IEEE Antennas and Wireless Propag. Lett.*, Vol. 19, No. 5, 796–800, 2020.
2. Gautam, V. A. K., L. Kumar, B. K. Kanaujia, and K. Rambabu, "Design of compact F-shaped slot triple-band antenna for WLAN/WiMAX applications," *IEEE Trans. Antennas and Propag.*, Vol. 64, No. 3, 1101–1105, 2016.
3. Zhang, H., Y.-C. Jiao, T. Ni, and W.-L. Liang, "Broadband circularly polarised antenna with asymmetric ground and L-shaped strips," *Electron. Lett.*, Vol. 50, 1660–1662, 2014.
4. Wei, W. Y., Y. Shi, Q. W. Wu, Z. K. Meng, and Z. Q. Liu, "Wideband composite planar spiral antenna for generation of tunable angular momentum wave," *Opt. Express*, Vol. 29, No. 3, 3754–3763, 2021.
5. Jung, J. S., J. N. Lee, J. M. Kim, and J. K. Park, "An UHF RFID reader antenna with multitag identification for extremely low-temperature medical systems," *International Journal of Antennas and Propagation*, Vol. 2020, Article ID 2482961, 11 pages, 2020.
6. Wang, L., W.-X. Fang, W.-H. Shao, B. Yao, Y. Huang, and Y.-F. En, "Broadband circularly polarized cross-dipole antenna with multiple modes," *IEEE Access*, Vol. 8, 66489–66494, 2020.

7. Yuan, Y., Q. Wu, S. N. Burokur, and K. Zhang, "Chirality-assisted phase metasurface for circular polarization preservation and independent hologram imaging in microwave region," *IEEE Transactions on Microwave Theory and Techniques*, Early Access, 1–14, 2023.
8. Li, J., Y. Yuan, G. Yang, Q. Wu, W. Zhang, S. N. Burokur, and K. Zhang, "Hybrid dispersion engineering based on chiral metamirror," *Laser Photonics Rev.*, Vol. 17, 2200777, 2023.
9. Gorai, A., M. Pal, and R. Ghatak, "A compact fractal-shaped antenna for ultrawideband and bluetooth wireless systems with WLAN rejection functionality," *IEEE Antennas and Wireless Propag. Lett.*, Vol. 16, 2163–2166, 2017.
10. Bhaskar, S., M. G. Siddiqui, S. Singhal, and A. Bansal, "Miniaturized circularly polarized vicsekcross-shaped slot antenna for UHF-RFID reader handset applications," *IEEE J. Radio Freq. Identif.*, Vol. 6, 515–523, 2022.
11. Xu, Y., K.-M. Luk, A. Li, and J. Sun, "A novel compact magneto-electric dipole antenna for millimeter-wave beam steering applications," *IEEE Trans. Veh. Technol.*, Vol. 70, No. 11, 11772–11783, Nov. 2021.
12. Fan, T.-Q., B. Jiang, R. Liu, J. Xiu, Y. Lin, and H. Xu, "A novel double U-slot microstrip patch antenna design for low-profile and broad bandwidth applications," *IEEE Trans. Antennas and Propag.*, Vol. 70, No. 4, 2543–2549, Apr. 2022.
13. Radavaram, S. and M. Pour, "Wideband radiation reconfigurable microstrip patch antenna loaded with two inverted U-slots," *IEEE Trans. Antennas and Propag.*, Vol. 67, No. 3, 1501–1508, Mar. 2019.
14. Yan, B., W. Sheng, L. Sun, and Z. N. Chen, "Wideband wide-scanning planar triangular-lattice phased array with substrate-integrated cavity-backed U-slot patches," *IEEE Trans. Antennas and Propag.*, Vol. 69, No. 9, 6082–6086, Sept. 2021.